Check for updates

Geophysical Research Letters

RESEARCH LETTER
10.1029/2022GL099470

Key Points:

- Satellite formaldehyde (HCHO) columns correlate moderately to highly with night-time light radiance and population density in most major Asian countries
- A monotonic response between anthropogenic non-methane volatile organic compound (NMVOC) emissions and urbanization may exist in Asia, with no apparent turnover yet
- TROPOspheric Monitoring Instrument HCHO column is confirmed as a reliable proxy of anthropogenic NMVOC emissions in Asia

Supporting Information:

Supporting Information may be found in the online version of this article.

Correspondence to:

L. Zhu,
zhul3@sustech.edu.cn

Citation:

Pu, D., Zhu, L., De Smedt, I., Li, X., Sun, W., Wang, D., et al. (2022). Response of anthropogenic volatile organic compound emissions to urbanization in Asia probed with TROPOMI and VIIRS satellite observations. *Geophysical Research Letters*, *49*, e2022GL099470. https://doi.org/10.1029/2022GL099470

Received 9 MAY 2022
Accepted 12 SEP 2022

Author Contributions:

Conceptualization: Lei Zhu
Data curation: Isabelle De Smedt
Formal analysis: Dongchuan Pu
Investigation: Shuai Sun
Methodology: Dongchuan Pu, Lei Zhu, Xicheng Li, Wenfu Sun
Project Administration: Lei Zhu
Resources: Lei Zhu
Software: Dongchuan Pu
Visualization: Dongchuan Pu

© 2022 The Authors.
This is an open access article under the terms of the Creative Commons Attribution-NonCommercial License, which permits use, distribution and reproduction in any medium, provided the original work is properly cited and is not used for commercial purposes.

Response of Anthropogenic Volatile Organic Compound Emissions to Urbanization in Asia Probed With TROPOMI and VIIRS Satellite Observations

Dongchuan Pu[1,2], Lei Zhu[2,3], Isabelle De Smedt[4], Xicheng Li[2], Wenfu Sun[2,4], Dakang Wang[2], Song Liu[2], Juan Li[1,2], Lei Shu[2], Yuyang Chen[2], Shuai Sun[2], Xiaoxing Zuo[2], Weitao Fu[2], Peng Xu[2], Xin Yang[2,3], and Tzung-May Fu[2,3]

[1]School of Environment, Harbin Institute of Technology, Harbin, China, [2]School of Environmental Science and Engineering, Southern University of Science and Technology, Shenzhen, China, [3]Guangdong Provincial Observation and Research Station for Coastal Atmosphere and Climate of the Greater Bay Area, Shenzhen, China, [4]Division of Atmospheric Composition, Royal Belgian Institute for Space Aeronomy, Brussels, Belgium

Abstract Emissions of air pollutants and their precursors in urban air closely relate to urbanization involving economic development, population growth, and industrialization. Here we use formaldehyde (HCHO) columns from the TROPOspheric Monitoring Instrument (TROPOMI), night-time light (NTL) radiance from the Visible Infrared Imaging Radiometer Suite, and population density data as respective proxies to explore how anthropogenic non-methane volatile organic compound (NMVOC) emissions evolve with urbanization in Asia. HCHO columns correlate moderately to highly ($0.64 \leq r \leq 0.99$) with the NTL radiance within most major Asian countries. On both national (across Asia) and provincial scales (within China), HCHO columns increase monotonically with NTL radiance or population density with a log-linear pattern, implying anthropogenic NMVOC emissions in Asia may similarly respond to urbanization with no apparent turnover yet. Our study confirms TROPOMI HCHO columns as a proxy of anthropogenic NMVOC emissions.

Plain Language Summary We use multi-source satellite remote sensing data and population density data to examine how anthropogenic non-methane volatile organic compound (NMVOC) emissions evolve with urbanization in Asia. Anthropogenic NMVOC emissions (indicated by satellite formaldehyde columns) correlate moderately to highly with urbanization (indicated by night-time light or population density) within most major Asian countries. We find a monotonic response between anthropogenic NMVOC emissions and urbanization in Asia, with no apparent turnover yet.

1. Introduction

As one of the most severe environmental issues apace with urbanization, air pollution poses significant threats to public health and the ecosystem in populous Asia. Emissions of air pollutants and their precursors respond differently to urbanization (Ding et al., 2015; Geddes et al., 2016; Li et al., 2016; Sinha & Bhattacharya, 2016). For example, the response of SO_2 to urbanization (indicated by per-capita income) is an inverted U-shaped pattern (Stern, 2004), while $PM_{2.5}$ responses to urbanization (indicated by time) in a linear manner (van Donkelaar et al., 2015), neither has been found with clear drivers. The pattern for anthropogenic non-methane volatile organic compounds (NMVOCs) remains unclear in Asia, primarily due to uncertainties in the bottom-up estimations of NMVOC emissions. Here, we use formaldehyde (HCHO) columns from the newly launched TROPOspheric Monitoring Instrument (TROPOMI) satellite (Veefkind et al., 2012) as a proxy of NMVOC emissions, together with the Visible Infrared Imaging Radiometer Suite (VIIRS) (C. Cao et al., 2013) night-time light (NTL) data (Elvidge et al., 2017) and population density data (Doxsey-Whitfield et al., 2015) as measures of urbanization, to explore how anthropogenic NMVOC emissions evolve with urbanization across Asian countries.

Anthropogenic NMVOCs are major precursors of particulate matter and surface ozone in the urban air (Jin & Holloway, 2015; Seinfeld & Pandis, 2012). That being said, anthropogenic NMVOC emissions in Asia increased from 50.8 TgC in 2010 to 55.5 TgC in 2017, contributing significantly (~31%) to the global total emission (McDuffie et al., 2020). Urban NMVOCs in Asia are mainly emitted from industrial activities, transportation, and fuel use (Wang et al., 2014; Wei et al., 2011). Recently, anthropogenic NMVOC emissions are ramping up rapidly due to automobile, solvent, and paint usage (Kurokawa et al., 2013; Ohara et al., 2007).

19448007, 2022, 18, Downloaded from https://agupubs.onlinelibrary.wiley.com/doi/10.1029/2022GL099470 by South University Of Science, Wiley Online Library on [11/10/2022]. See the Terms and Conditions (https://onlinelibrary.wiley.com/terms-and-conditions) on Wiley Online Library for rules of use; OA articles are governed by the applicable Creative Commons License

Writing – original draft: Dongchuan Pu, Lei Zhu
Writing – review & editing: Dongchuan Pu, Lei Zhu, Isabelle De Smedt, Xicheng Li, Dakang Wang, Song Liu, Juan Li, Lei Shu, Yuyang Chen, Xiaoxing Zuo, Weitao Fu, Tzung-May Fu

Satellite HCHO columns have been widely used as a proxy of anthropogenic NMVOC emissions (Boeke et al., 2011; Fu et al., 2007; H. Cao et al., 2018; Souri et al., 2020; Stavrakou et al., 2015; Sun et al., 2021; Zhu, Jacob, et al., 2017; Zhu et al., 2020), because of the short atmospheric lifetime of HCHO (a few hours against oxidation and photolysis) and relatively high HCHO production yields from the oxidation of various highly reactive anthropogenic NMVOCs. In addition, satellite HCHO columns are sensitive to biogenic isoprene and monoterpenes emissions (Barkley et al., 2013; Curci et al., 2010; Millet et al., 2006, 2008; Palmer et al., 2003; Shim et al., 2005), with air temperature as the primary driver of the seasonal variations in HCHO columns (Duncan et al., 2009; Kaiser et al., 2018; Palmer et al., 2006; Zhu et al., 2014; Zhu, Mickley, et al., 2017). In this study, we use TROPOMI HCHO columns to probe the relationship between anthropogenic NMVOC emissions and urbanization in Asia at a high spatial resolution, as discussed below.

2. Data and Method

2.1. TROPOMI HCHO Columns

As a nadir-viewing hyperspectral spectrometer, TROPOMI is onboard the Copernicus Sentinel-5 Precursor platform, launched in October 2017. TROPOMI provides daily global coverage with a high spatial resolution of 7.0×3.5 km^2 (upgraded to 5.5×3.5 km^2 since August 2019) and signal-to-noise ratio (Veefkind et al., 2012) at a local cross-time of 13:30. TROPOMI HCHO product (De Smedt et al., 2018, 2021) has been validated against observations from the Multi-AXis Differential Optical Absorption Spectroscopy (MAX-DOAS) (Chan et al., 2020) and Fourier-transform infrared (FTIR) (Vigouroux et al., 2020) instruments. Meanwhile, intercomparison with Ozone Monitoring Instrument (OMI) monthly averaged HCHO columns suggests the retrieval consistency between OMI and TROPOMI (De Smedt et al., 2021). Therefore, TROPOMI HCHO products have been gradually applied to identify the sources of volatile organic compounds (VOCs) (Pakkattil et al., 2021; Xing et al., 2020) and their variations (Sun et al., 2021).

To ensure data quality, we use TROPOMI HCHO data from May–October (in 2018 and 2019), when HCHO columns are higher and satellite light paths are shorter. TROPOMI level-2 pixels are filtered based on cloud fractions (<30%), solar zenith angles (<60°), and quality assurance value (>0.5). We then regrid all qualified level-2 pixels during May–October in 2018 and 2019 onto the $0.05° \times 0.05°$($\sim 5 \times 5$ km^2) grids, built on our previous oversampling method (Sun et al., 2021; Zhu et al., 2014; Zhu, Jacob, et al., 2017; Zhu, Mickley, et al., 2017).

As shown in Figure 1 (panel a), the elevated HCHO columns over northern India and eastern China emphasize the significant impact of biogenic NMVOCs on the regional scale (H. Cao et al., 2018; Surl et al., 2018). We also see relatively high HCHO columns over urban areas in Asia, such as the Indo-Gangetic Plain, North China Plain, Pearl River Delta, and Hanoi, highlighting contributions from anthropogenic NMVOC emissions. This is due partly to NMVOC emissions from industrial activities and transportation, which account for more than 45% of the total NMVOC emissions in China and has been growing fast in India (Kurokawa et al., 2013).

2.2. VIIRS NTL Radiance

Previous studies have used NTL data as an indicator of urbanization, such as urban area expansion (Elvidge et al., 1999; Sutton, 2003) and economic development (Chen & Li, 2019; Levin & Duke, 2012; Levin & Zhang, 2017; Zhao et al., 2017). Following the annual composite approach suggested by Zhang et al. (2021), we compute the median of VIIRS monthly NTL radiance (Elvidge et al., 2017) in 2019 on the Google Earth Engine platform (Gorelick et al., 2017), and use it to measure urbanization levels in Asia (Figure 2a). Here, we use the median radiance to remove outliers introduced by wildfires.

High HCHO columns (Figure 1a) generally collocate with areas indicated by relatively high NTL radiance (Figure 2a), implying that human economic activities and NMVOC emissions are closely related. For instance, the developed eastern and coastal regions emit more NMVOCs than the less developed western and inland regions in China (Li et al., 2016), similar to the NTL spatial pattern in Figure 2a.

2.3. Spatial Sampling Method

To focus on anthropogenic NMVOCs, we select grid cells where (a) HCHO columns weakly depend on air temperature and (b) are not influenced by wildfires. The first criterion is to filter out biogenic-dominated grid

19448007, 2022, 18, Downloaded from https://agupubs.onlinelibrary.wiley.com/doi/10.1029/2022GL099470 by South University Of Science, Wiley Online Library on [11/10/2022]. See the Terms and Conditions (https://onlinelibrary.wiley.com/terms-and-conditions) on Wiley Online Library for rules of use; OA articles are governed by the applicable Creative Commons License

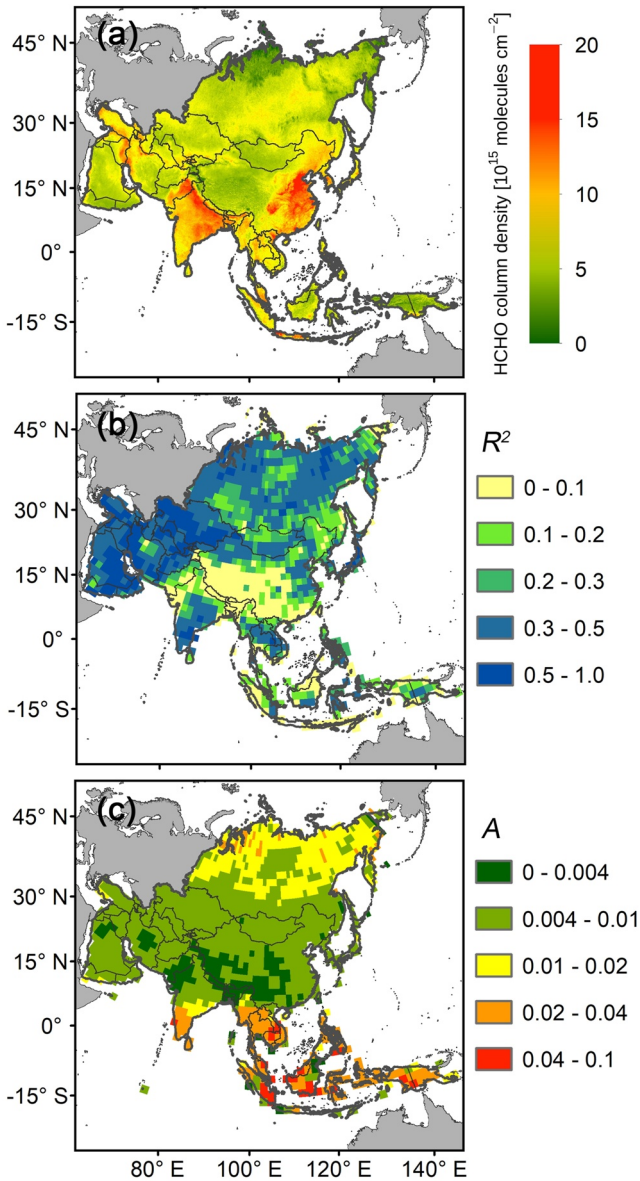

Figure 1. TROPOMI HCHO columns and temperature dependency over Asia. Panel (a) shows TROPOMI HCHO columns during May–October in 2018 and 2019 oversampled to a 0.05° × 0.05° (~5 × 5 km^2) grid resolution. Panel (b) shows the temperature dependency (determination coefficient, R^2) between monthly HCHO columns (Ω, in molecules cm^{-2}) and surface temperature (T, in K), calculated by fitting an exponential relationship ($\log_{10}\Omega = AT + B$, where A and B are fitting parameters) with data during May–October in 2018 and 2019. T is from MERRA-2 surface temperature (Gelaro et al., 2017). To obtain reliable statistics, Ω and T are regridded to a 2° × 2° grid resolution before the fitting. Panel (c) shows slope (A) fitted with the aforementioned exponential relationship.

cells. This is conducted by utilizing the exponential dependency of biogenic HCHO columns on air temperature (Duncan et al., 2009; Zhu et al., 2014; Zhu, Mickley, et al., 2017). Here we use NASA Modern-Era Retrospective Analysis for Research and Applications-2 (MERRA-2) (Gelaro et al., 2017) surface temperature to build localized exponential temperature dependency of HCHO columns (Figures 1b and 1c). We then exclude grid cells with strong biogenic influence ($R^2 > 0.5$ and $A > 0.05$) from further analysis. $R^2 > 0.5$ indicates a strong correlation between surface temperature and HCHO columns, and $A > 0.05$ indicates HCHO column significantly depends on surface temperature, either suggesting strong biogenic influence. Finally, we eliminate grid cells influenced by wildfire based on carbon monoxide emission flux (>1 × 10^{-6} kg m^{-2} yr^{-1}) from the Global Fire Emissions Database 4 (GFED 4) (van der Werf et al., 2017) in 2019.

To focus on urban areas, we limit our further analysis to previously resulting grid cells containing at least one urban site. Here we survey 37,320 urban sites in Asia based on the geolocation of administrative, residential, and commercial centers, following Zhang et al. (2021). The accuracy (96%) of the defined urban sites is verified by visually checking randomly selected 500 sites against corresponding high-resolution Google Earth images. From Figure 2b, we see that urban sites are generally located at grid cells with high NTL radiance, supporting using NTL radiance as a measure of urbanization.

3. Results and Discussions

Our analysis begins with the relationship between anthropogenic NMVOC emissions (indicated by TROPOMI HCHO columns) and urbanization (indicated by NTL radiance and population density) within each major Asian country (hereafter defined as countries with more than 200 urban sites defined in Section 2.3). Figure 3 demonstrates a significant (p-value ≤ 0.05) positive correlation between TROPOMI HCHO columns and the NTL radiance in Japan, Indonesia, the Philippines, and India, the top four countries with the highest correlation coefficients. In total, we find significant linear relationships in 19 of 24 major Asian countries, with correlation coefficients (r) ranging from 0.64 to 0.99 (Table S1 in Supporting Information S1). Similarly, TROPOMI HCHO columns correlate closely with population density in major Asian countries ($0.70 \le r \le 0.99$), due to the linear relationship between NTL radiance and population density ($0.76 \le r \le 0.99$).

We also explore the relationship between TROPOMI HCHO columns and bottom-up anthropogenic VOC emissions within major Asian countries using the Emissions Database for Global Atmospheric Research (EDGAR) inventory (Huang et al., 2017). Following the mass balance approach proposed by Palmer et al. (2003) and Zhu et al. (2014), we select five highly reactive VOCs (ethene, propene, isoprene, monoterpenes, and HCHO) with atmospheric lifetimes shorter than 2 hr (Table S2 in Supporting Information S1) to roughly estimate EDGAR-based HCHO columns based on local emission fluxes. The moderate-to-high linear relationships ($0.65 \le r \le 0.89$; Table S1 in Supporting Information S1) between EDGAR-based and TROPOMI HCHO columns confirm the reliability of satellite HCHO columns as a proxy of anthropogenic NMVOC emissions among countries, acknowledging the potential underestimation of HCHO produced by long-lived NMVOCs.

The linear relationships between EDGAR-based and TROPOMI HCHO columns also imply a way to identify possible drivers of the differences in TROPOMI HCHO and NTL radiance (and population density) relationship

19448007, 2022, 18, Downloaded from https://agupubs.onlinelibrary.wiley.com/doi/10.1029/2022GL099470 by South University Of Science, Wiley Online Library on [11/10/2022]. See the Terms and Conditions (https://onlinelibrary.wiley.com/terms-and-conditions) on Wiley Online Library for rules of use; OA articles are governed by the applicable Creative Commons License

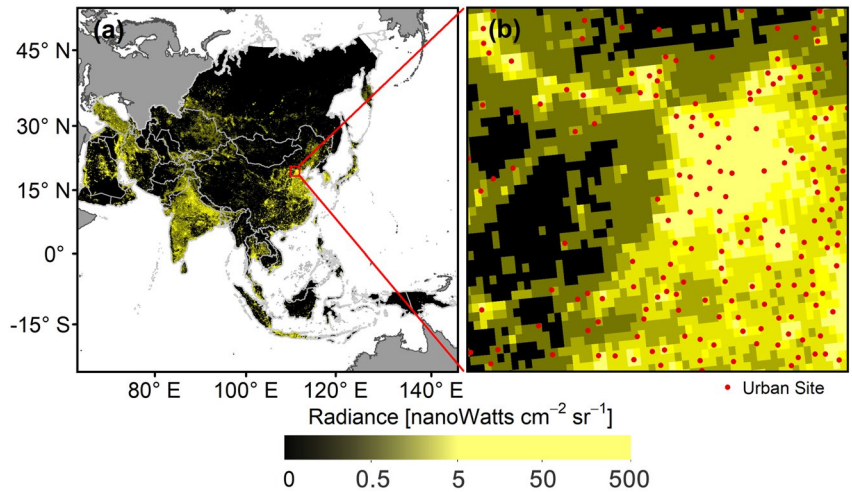

Figure 2. Annual night-time light (NTL) radiance over Asia according to VIIRS. Panel (a) shows VIIRS annual NTL radiance in 2019 at a resolution of 0.05° × 0.05° (~5 × 5 km^2), computed based on the median synthesis method provided by the Google Earth Engine. Panel (b) zooms in a region near Beijing-Tianjin-Hebei urban agglomeration, the red box in panel (a). Red dots are urban sites defined as administrative (province, city, and county domains), residual, and commercial centers (details in Section 2.3).

among Asian countries (Figure 1; Table S1 in Supporting Information S1) by examine contributions from various species and sectors (Table S3 in Supporting Information S1). For instance, Japan has a much higher correlation coefficient (0.99) than Bangladesh (0.77). We hypothesize such a difference is caused by different contributions from emission sectors (Table S3 in Supporting Information S1), including industry (74% *vs*. 41%), residential

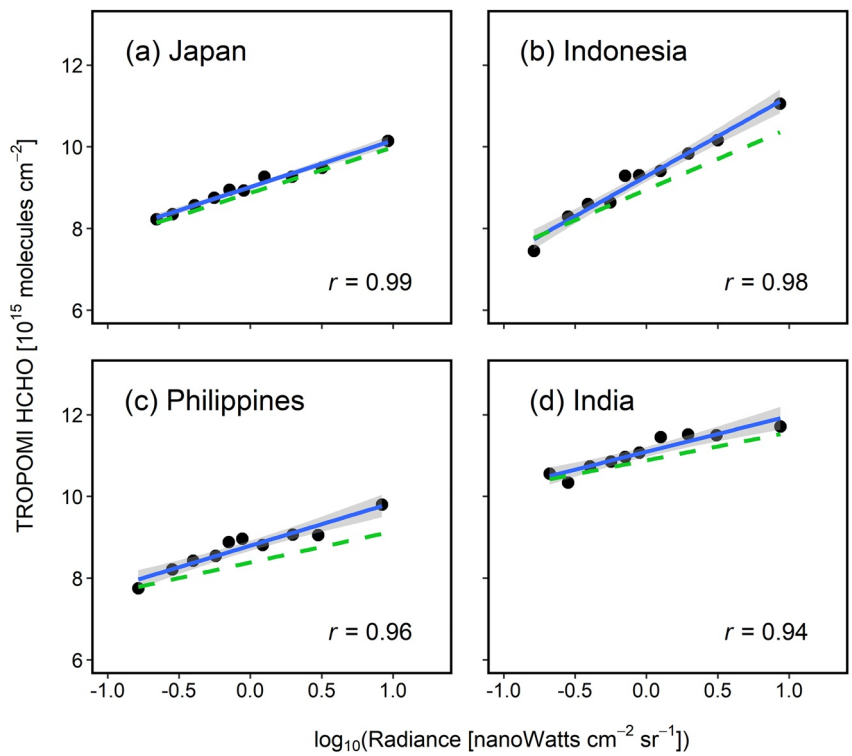

Figure 3. The relationship between HCHO columns and VIIRS NTL radiance. Panels (a–d) indicates Japan, Indonesia, the Philippines, and India in order. In each panel, a point represents the mean HCHO columns at a specific NTL radiance bin for all urban grid cells (defined in Section 2.3) within that country. The blue line shows the simple linear regression line, with a gray area enveloping the 95% confidence interval of the mean response. Pearson correlation coefficients (*r*) are also inserted. The green dashed line represents the simple linear regression line after excluding the impact of spatial variations of NO_x emissions on HCHO columns (details in Text S2 in Supporting Information S1).

19448007, 2022, 18, Downloaded from https://agupubs.onlinelibrary.wiley.com/doi/10.1029/2022GL099470 by South University Of Science, Wiley Online Library on [11/10/2022]. See the Terms and Conditions (https://onlinelibrary.wiley.com/terms-and-conditions) on Wiley Online Library for rules of use; OA articles are governed by the applicable Creative Commons License

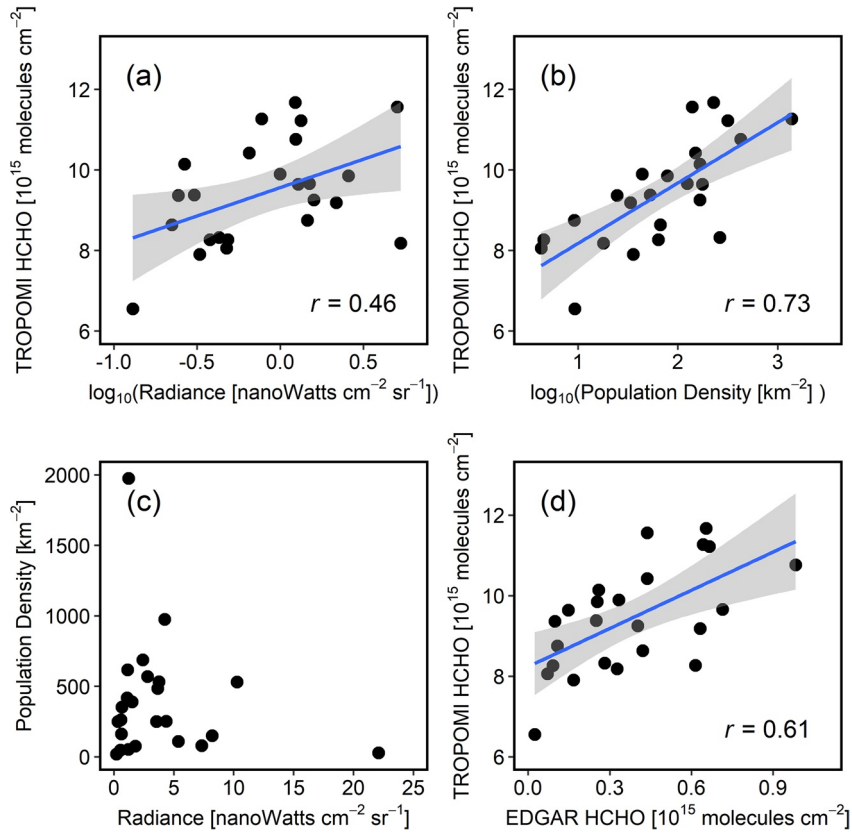

Figure 4. The response of HCHO columns to NTL radiance (panel a) and population density (panel b). The relationship between NTL radiance and population density (panel c), and between TROPOMI and EDGAR-based HCHO columns (panel d). Each point represents the national-averaged TROPOMI HCHO columns, NTL radiance, population density, or EDGAR-based HCHO columns for all urbanization grid cells (Section 2.3) in a specific country. The blue line is a log-linear (panels a and b) or linear (panels d) fitting, with the gray area enveloping the 95% confidence interval of the mean response. Pearson correlation coefficients (r) are also inserted (panels a, b, and d).

(4% *vs*. 23%), and agriculture (5% *vs*. 16%) – NTL could be more likely relevant to industry rather than non-point residential and agriculture sources. Meanwhile, the slope discrepancy between Russia and Uzbekistan (Table S1 in Supporting Information S1) may be traced to speciations of emitted VOCs. The lower slope in Russia could be driven by lower contributions of secondary production (49% *vs*. 99%; Table S3 in Supporting Information S1) from species with higher HCHO yields, including ethene, propene, and isoprene (Table S2 in Supporting Information S1). Nevertheless, more concrete and mechanistic drivers deserve further studies.

To encapsulate the spatial complexity within a country, we compute the national-averaged TROPOMI HCHO columns, NTL radiance, and population density. We fit a log-linear regression, given the highly skewed NTL radiance (skewness 2.81) and population density data (skewness 19.5). Figures 4a and 4b show how anthropogenic NMVOC emissions (indicated by HCHO columns) vary with urbanization (indicated by NTL radiance and population density) on the national scale. The log-linear relationship is weak (r = 0.46, p-value = 0.02) between HCHO columns and NTL radiance, but much stronger between HCHO and population density (r = 0.73, p-value < 0.01).

Population growth in Asia results in higher demand for transportation, electricity, and solvent usage, all contributing to NMVOCs emissions and thus HCHO columns. However, such linearity is not necessarily reflected by examining the relationship between HCHO columns and NTL radiance (Figure 4c). This likely suggests population density as an overall indicator of NMVOCs emissions from industry, ground transport, and residential sectors, whereas NTL radiation is more relevant to electrical energy consumption (Chen & Li, 2019) than other sectors. Nevertheless, given the advantages of real-time updates, large scanning range, and quick response, satellite NTL radiance data still have great potential to characterize urbanization. Furthermore,

19448007, 2022, 18, Downloaded from https://agupubs.onlinelibrary.wiley.com/doi/10.1029/2022GL099470 by South University Of Science, Wiley Online Library on [11/10/2022]. See the Terms and Conditions (https://onlinelibrary.wiley.com/terms-and-conditions) on Wiley Online Library for rules of use; OA articles are governed by the applicable Creative Commons License

the linearity between TROPOMI and EDGAR-based HCHO columns ($r = 0.61$, p-value < 0.01) confirms TROPOMI HCHO columns again as a reliable proxy of anthropogenic NMVOC emissions, at least on the national scale (Figure 4d).

Following the same approach, we analyze how anthropogenic NMVOC emissions vary with urbanization on the provincial scale in China (Figure S1 in Supporting Information S1). China emits the most anthropogenic NMVOCs worldwide, accounting for ~15% of the global total emission (Wei et al., 2011), with major emission sectors from solvent usage, industrial processes, road vehicles, and fuel combustion. Similar to the national relationship between anthropogenic NMVOC emissions and urbanization (Figures 4a and 4b), provincial HCHO columns logarithmically depend on urbanization, with a higher correlation with population density ($r = 0.75$, p-value < 0.01) than NTL radiance ($r = 0.28$, p-value $= 0.10$). This implies a general linear pattern between anthropogenic NMVOC emissions and urbanization may exist, regardless of geographical differences. However, we may not be able to make quantitative predictions of such a linear trend in the future based on current observations.

The dependency of HCHO yields from NMVOCs on NO_x emissions is nonlinear (Miller et al., 2017; Valin et al., 2016; Wolfe et al., 2016), thus complicating the relationships between anthropogenic NMVOC emissions and HCHO columns. We conduct five GEOS-Chem (nested version, $0.5° \times 0.625°$) sensitivity simulations (Text S1 in Supporting Information S1) along with using TROPOMI NO_2 data (van Geffen et al., 2020; Text S2 in Supporting Information S1) to quantify such a dependency over Asia. We find that excluding anthropogenic NO_x emissions, on average, reduces HCHO columns by up to ~40% in Eastern Asia and by ~30% in Central Asia (Figure S2 in Supporting Information S1). We further quantify the impact of spatial variations of NO_x emissions on HCHO columns (Text S2 in Supporting Information S1), and find that such an impact is slight in most Asia countries. For example, the slope is reduced by 3% in Japan, 19% in India, and 22% in Indonesia (Figure 3), after accounting for the spatial variations of NO_x emissions. The largest impact (36%) is seen in Malaysia. Therefore, we argue that linear patterns between TROPOMI HCHO columns and NTL radiance (Figures 3 and 4; Table S1 in Supporting Information S1) may be primarily driven by gradients of NMVOC rather than NO_x emissions. Nevertheless, we acknowledge that NO_x and NMVOC emissions from various sectors may vary spatially, and localized HCHO-NMVOCs relationships deserve future exploration.

4. Conclusion

We have used TROPOMI, VIIRS satellite observations, and population density data to explore how anthropogenic non-methane volatile organic compound (NMVOC) emissions evolve with urbanization in Asia. We find HCHO columns (an indicator of anthropogenic NMVOC emissions) correlate moderately to highly ($0.64 \leq r \leq 0.99$) with night-time light (NTL) radiance (an indicator of urbanization) within major Asian countries. TROPOMI HCHO column is confirmed as a reliable proxy of anthropogenic NMVOC emissions in Asia. Our study suggests a linear response between anthropogenic NMVOC emissions and urbanization in Asia currently, with no apparent turnover yet.

Data Availability Statement

The TROPOMI HCHO, NO_2, and MERRA-2 products used in this study are from the NASA Goddard Earth Sciences Data and Information Services Center (https://disc.gsfc.nasa.gov/datasets/S5P_L2__HCHO___1/summary?keywords=TROPOMI%20HCHO, https://disc.gsfc.nasa.gov/datasets/S5P_L2__NO2____HiR_1/summary?keywords=NO2, and https://disc.gsfc.nasa.gov/datasets/M2T1NXSLV_5.12.4/summary?keywords=MERRA-2). The VIIRS night light data are from NOAA National Centers for Environmental Information (NCEI) (https://ngdc.noaa.gov/eog/viirs/download_ut_mos.html). The population density data in 2015 are from the NASA Socioeconomic Data and Applications Center (SEDAC) (http://dx.doi.org/10.7927/H4ST7MRB). The EDGAR data are from European Union Joint Research Centre (https://edgar.jrc.ec.europa.eu/dataset_htap_v3). Oversampling code and plotting scripts are available at: https://zenodo.org/record/6843869%23.YtJMLXZByUk.

19448007, 2022, 18, Downloaded from https://agupubs.onlinelibrary.wiley.com/doi/10.1029/2022GL099470 by South University Of Science, Wiley Online Library on [11/10/2022]. See the Terms and Conditions (https://onlinelibrary.wiley.com/terms-and-conditions) on Wiley Online Library for rules of use; OA articles are governed by the applicable Creative Commons License

Acknowledgments
This work is funded by the Key-Area Research and Development Program of Guangdong Province (2020B1111360001), Guangdong Basic and Applied Basic Research Foundation (2021A1515110713), Guangdong University Research Project Science Team (2021KCXTD004), Guangdong Basic and Applied Basic Research Fund Committee (2020B1515130003), Guangdong University Youth Innovation Talent Project (2020KQNCX066), Shenzhen Science and Technology Program (JCYJ20210324104604012). This work is supported by the Center for Computational Science and Engineering at Southern University of Science and Technology. The TROPOMI HCHO product developments are funded by the Copernicus Sentinel-5 Precursor Mission Performance Centre (S5p MPC), contracted by the European Space Agency (ESA/ESRIN, contract no. 4000117151/16/I-LG) and supported by the Belgian Federal Science Policy Office (BELSPO), the Royal Belgian Institute for Space Aeronomy (BIRA-IASB) and the German Aerospace Centre (DLR).

References

Barkley, M. P., Smedt, I. D., Van Roozendael, M., Kurosu, T. P., Chance, K., Arneth, A., et al. (2013). Top-down isoprene emissions over tropical South America inferred from SCIAMACHY and OMI formaldehyde columns. *Journal of Geophysical Research: Atmospheres*, *118*(12), 6849–6868. https://doi.org/10.1002/jgrd.50552

Boeke, N. L., Marshall, J. D., Alvarez, S., Chance, K. V., Fried, A., Kurosu, T. P., et al. (2011). Formaldehyde columns from the Ozone Monitoring Instrument: Urban versus background levels and evaluation using aircraft data and a global model. *Journal of Geophysical Research*, *116*(D5), D05303. https://doi.org/10.1029/2010JD014870

Cao, C., De Luccia, F. J., Xiong, X., Wolfe, R., & Weng, F. (2013). Early on-orbit performance of the visible infrared imaging radiometer suite onboard the Suomi National Polar-Orbiting Partnership (S-NPP) satellite. *IEEE Transactions on Geoscience Remote sensing of environment*, *52*(2), 1142–1156. https://doi.org/10.1109/TGRS.2013.2247768

Cao, H., Fu, T.-M., Zhang, L., Henze, D. K., Miller, C. C., Lerot, C., et al. (2018). Adjoint inversion of Chinese non-methane volatile organic compound emissions using space-based observations of formaldehyde and glyoxal. *Atmospheric Chemistry and Physics*, *18*(20), 15017–15046. https://doi.org/10.5194/acp-18-15017-2018

Chan, K. L., Wiegner, M., van Geffen, J., De Smedt, I., Alberti, C., Cheng, Z., et al. (2020). MAX-DOAS measurements of tropospheric NO_2 and HCHO in Munich and the comparison to OMI and TROPOMI satellite observations. *Atmospheric Measurement Techniques*, *13*(8), 4499–4520. https://doi.org/10.5194/amt-13-4499-2020

Chen, J. J., & Li, L. (2019). Regional economic activity derived from MODIS data: A comparison with DMSP/OLS and NPP/VIIRS nighttime light data. *IEEE Journal of Selected Topics in Applied Earth Observations and Remote Sensing*, *12*(8), 3067–3077. https://doi.org/10.1109/jstars.2019.2915646

Curci, G., Palmer, P. I., Kurosu, T. P., Chance, K., & Visconti, G. (2010). Estimating European volatile organic compound emissions using satellite observations of formaldehyde from the Ozone Monitoring Instrument. *Atmospheric Chemistry and Physics*, *10*(23), 11501–11517. https://doi.org/10.5194/acp-10-11501-2010

De Smedt, I., Pinardi, G., Vigouroux, C., Compernolle, S., Bais, A., Benavent, N., et al. (2021). Comparative assessment of TROPOMI and OMI formaldehyde observations and validation against MAX-DOAS network column measurements. *Atmospheric Chemistry and Physics*, *21*(16), 12561–12593. https://doi.org/10.5194/acp-21-12561-2021

De Smedt, I., Theys, N., Yu, H., Danckaert, T., Lerot, C., Compernolle, S., et al. (2018). Algorithm theoretical baseline for formaldehyde retrievals from S5P TROPOMI and from the QA4ECV project. *Atmospheric Measurement Techniques*, *11*(4), 2395–2426. https://doi.org/10.5194/amt-11-2395-2018

Ding, L., Zhao, W., Huang, Y., Cheng, S., & Liu, C. (2015). Research on the coupling coordination relationship between urbanization and the air environment: A case study of the area of Wuhan. *Atmosphere*, *6*(10), 1539–1558. https://doi.org/10.3390/atmos6101539

Doxsey-Whitfield, E., MacManus, K., Adamo, S. B., Pistolesi, L., Squires, J., Borkovska, O., & Baptista, S. R. (2015). Taking advantage of the improved availability of census data: A first look at the gridded population of the world, version 4. *Papers in Applied Geography*, *1*(3), 226–234. https://doi.org/10.1080/23754931.2015.1014272

Duncan, B. N., Yoshida, Y., Damon, M. R., Douglass, A. R., & Witte, J. C. (2009). Temperature dependence of factors controlling isoprene emissions. *Geophysical Research Letters*, *36*(5), L05813. https://doi.org/10.1029/2008GL037090

Elvidge, C. D., Baugh, K., Zhizhin, M., Hsu, F. C., & Ghosh, T. (2017). VIIRS night-time lights. *International Journal of Remote Sensing*, *38*(21), 5860–5879. https://doi.org/10.1080/01431161.2017.1342050

Elvidge, C. D., Baugh, K. E., Dietz, J. B., Bland, T., Sutton, P. C., & Kroehl, H. W. (1999). Radiance calibration of DMSP-OLS low-light imaging data of human settlements. *Remote Sensing of Environment*, *68*(1), 77–88. https://doi.org/10.1016/S0034-4257(98)00098-4

Fu, T. M., Jacob, D. J., Palmer, P. I., Chance, K., Wang, Y. X., Barletta, B., et al. (2007). Space-based formaldehyde measurements as constraints on volatile organic compound emissions in east and south Asia and implications for ozone. *Journal of Geophysical Research*, *112*(D6), D06312. https://doi.org/10.1029/2006JD007853

Geddes, J. A., Martin, R. V., Boys, B. L., & van Donkelaar, A. (2016). Long-term trends worldwide in ambient NO_2 concentrations inferred from satellite observations. *Environmental Health Perspectives*, *124*(3), 281–289. https://doi.org/10.1289/ehp.1409567

Gelaro, R., McCarty, W., Suárez, M. J., Todling, R., Molod, A., Takacs, L., et al. (2017). The modern-era retrospective analysis for research and applications, version 2 (MERRA-2). *Journal of Climate*, *30*(14), 5419–5454. https://doi.org/10.1175/JCLI-D-16-0758.1

Gorelick, N., Hancher, M., Dixon, M., Ilyushchenko, S., Thau, D., & Moore, R. (2017). Google Earth Engine: Planetary-scale geospatial analysis for everyone. *Remote Sensing of Environment*, *202*, 18–27. https://doi.org/10.1016/j.rse.2017.06.031

Huang, G., Brook, R., Crippa, M., Janssens-Maenhout, G., Schieberle, C., Dore, C., et al. (2017). Speciation of anthropogenic emissions of non-methane volatile organic compounds: A global gridded data set for 1970–2012. *Atmospheric Chemistry and Physics*, *17*(12), 7683–7701. https://doi.org/10.5194/acp-17-7683-2017

Jin, X. M., & Holloway, T. (2015). Spatial and temporal variability of ozone sensitivity over China observed from the Ozone Monitoring Instrument. *Journal of Geophysical Research: Atmospheres*, *120*(14), 7229–7246. https://doi.org/10.1002/2015jd023250

Kaiser, J., Jacob, D. J., Zhu, L., Travis, K. R., Fisher, J. A., González Abad, G., et al. (2018). High-resolution inversion of OMI formaldehyde columns to quantify isoprene emission on ecosystem-relevant scales: Application to the southeast US. *Atmospheric Chemistry and Physics*, *18*(8), 5483–5497. https://doi.org/10.5194/acp-18-5483-2018

Kurokawa, J., Ohara, T., Morikawa, T., Hanayama, S., Janssens-Maenhout, G., Fukui, T., et al. (2013). Emissions of air pollutants and greenhouse gases over Asian regions during 2000–2008: Regional Emission inventory in ASia (REAS) version 2. *Atmospheric Chemistry and Physics*, *13*(21), 11019–11058. https://doi.org/10.5194/acp-13-11019-2013

Levin, N., & Duke, Y. (2012). High spatial resolution night-time light images for demographic and socio-economic studies. *Remote Sensing of Environment*, *119*, 1–10. https://doi.org/10.1016/j.rse.2011.12.005

Levin, N., & Zhang, Q. L. (2017). A global analysis of factors controlling VIIRS nighttime light levels from densely populated areas. *Remote Sensing of Environment*, *190*, 366–382. https://doi.org/10.1016/j.rse.2017.01.006

Li, G., Fang, C., Wang, S., & Sun, S. (2016). The effect of economic growth, urbanization, and industrialization on fine particulate matter ($PM_{2.5}$) concentrations in China. *Environmental Science & Technology*, *50*(21), 11452–11459. https://doi.org/10.1021/acs.est.6b02562

McDuffie, E. E., Smith, S. J., O'Rourke, P., Tibrewal, K., Venkataraman, C., Marais, E. A., et al. (2020). A global anthropogenic emission inventory of atmospheric pollutants from sector-and fuel-specific sources (1970–2017): An application of the community emissions data system (CEDS). *Earth System Science Data*, *12*(4), 3413–3442. https://doi.org/10.5194/essd-12-3413-2020

Miller, C. C., Jacob, D. J., Marais, E. A., Yu, K. R., Travis, K. R., Kim, P. S., et al. (2017). Glyoxal yield from isoprene oxidation and relation to formaldehyde: Chemical mechanism, constraints from SENEX aircraft observations, and interpretation of OMI satellite data. *Atmospheric Chemistry and Physics*, *17*(14), 8725–8738. https://doi.org/10.5194/acp-17-8725-2017

19448007, 2022, 18, Downloaded from https://agupubs.onlinelibrary.wiley.com/doi/10.1029/2022GL099470 by South University Of Science, Wiley Online Library on [11/10/2022]. See the Terms and Conditions (https://onlinelibrary.wiley.com/terms-and-conditions) on Wiley Online Library for rules of use; OA articles are governed by the applicable Creative Commons License

Millet, D. B., Jacob, D. J., Boersma, K. F., Fu, T.-M., Kurosu, T. P., Chance, K., et al. (2008). Spatial distribution of isoprene emissions from North America derived from formaldehyde column measurements by the OMI satellite sensor. *Journal of Geophysical Research*, *113*(D2), D02307. https://doi.org/10.1029/2007JD008950

Millet, D. B., Jacob, D. J., Turquety, S., Hudman, R. C., Wu, S., Fried, A., et al. (2006). Formaldehyde distribution over North America: Implications for satellite retrievals of formaldehyde columns and isoprene emission. *Journal of Geophysical Research*, *111*(D24), D24S02. https://doi.org/10.1029/2005JD006853

Ohara, T., Akimoto, H., Kurokawa, J., Horii, N., Yamaji, K., Yan, X., & Hayasaka, T. (2007). An Asian emission inventory of anthropogenic emission sources for the period 1980–2020. *Atmospheric Chemistry and Physics*, *7*(16), 4419–4444. https://doi.org/10.5194/acp-7-4419-2007

Pakkattil, A., Muhsin, M., & Varma, M. K. R. (2021). COVID-19 lockdown: Effects on selected volatile organic compound (VOC) emissions over the major Indian metro cities. *Urban Climate*, *37*, 100838. https://doi.org/10.1016/j.uclim.2021.100838

Palmer, P. I., Abbot, D. S., Fu, T.-M., Jacob, D. J., Chance, K., Kurosu, T. P., et al. (2006). Quantifying the seasonal and interannual variability of North American isoprene emissions using satellite observations of the formaldehyde column. *Journal of Geophysical Research*, *111*(D12), D12315. https://doi.org/10.1029/2005JD006689

Palmer, P. I., Jacob, D. J., Fiore, A. M., Martin, R. V., Chance, K., & Kurosu, T. P. (2003). Mapping isoprene emissions over North America using formaldehyde column observations from space. *Journal of Geophysical Research*, *108*(D6), 2002JD002153. https://doi.org/10.1029/2002JD002153

Seinfeld, J. H., & Pandis, S. N. (2012). *Atmospheric chemistry and physics: From air pollution to climate change*. Wiley.

Shim, C., Wang, Y., Choi, Y., Palmer, P. I., Abbot, D. S., & Chance, K. (2005). Constraining global isoprene emissions with Global Ozone Monitoring Experiment (GOME) formaldehyde column measurements. *Journal of Geophysical Research*, *110*(D24), D24301. https://doi.org/10.1029/2004JD005629

Sinha, A., & Bhattacharya, J. (2016). Environmental kuznets curve estimation for NO_2 emission: A case of Indian cities. *Ecological Indicators*, *67*, 1–11. https://doi.org/10.1016/j.ecolind.2016.02.025

Souri, A. H., Nowlan, C. R., González Abad, G., Zhu, L., Blake, D. R., Fried, A., et al. (2020). An inversion of NO_x and non-methane volatile organic compound (NMVOC) emissions using satellite observations during the KORUS-AQ campaign and implications for surface ozone over East Asia. *Atmospheric Chemistry and Physics*, *20*(16), 9837–9854. https://doi.org/10.5194/acp-20-9837-2020

Stavrakou, T., Müller, J.-F., Bauwens, M., Smedt, I. D., Van Roozendael, M., Mazière, M. D., et al. (2015). How consistent are top-down hydrocarbon emissions based on formaldehyde observations from GOME-2 and OMI? *Atmospheric Chemistry and Physics*, *15*(20), 11861–11884. https://doi.org/10.5194/acp-15-11861-2015

Stern, D. (2004). The rise and fall of the environmental Kuznets curve. *World Development*, *32*(8), 1419–1439. https://doi.org/10.1016/j.worlddev.2004.03.004

Sun, W., Zhu, L., De Smedt, I., Bai, B., Pu, D., Chen, Y., et al. (2021). Global significant changes in formaldehyde (HCHO) columns observed from space at the early stage of the COVID-19 pandemic. *Geophysical Research Letters*, *48*(4), 2e020GL091265. https://doi.org/10.1029/2020GL091265

Surl, L., Palmer, P. I., & González Abad, G. (2018). Which processes drive observed variations of HCHO columns over India? *Atmospheric Chemistry and Physics*, *18*(7), 4549–4566. https://doi.org/10.5194/acp-18-4549-2018

Sutton, P. C. (2003). A scale-adjusted measure of "urban sprawl" using nighttime satellite imagery. *Remote Sensing of Environment*, *86*(3), 353–369. https://doi.org/10.1016/S0034-4257(03)00078-6

Valin, L. C., Fiore, A. M., Chance, K., & Abad, G. G. (2016). The role of OH production in interpreting the variability of CH_2O columns in the southeast US. *Journal of Geophysical Research: Atmospheres*, *121*(1), 478–493. https://doi.org/10.1002/2015jd024012

van der Werf, G. R., Randerson, J. T., Giglio, L., van Leeuwen, T. T., Chen, Y., Rogers, B. M., et al. (2017). Global fire emissions estimates during 1997–2016. *Earth System Science Data*, *9*(2), 697–720. https://doi.org/10.5194/essd-9-697-2017

van Donkelaar, A., Martin, R. V., Brauer, M., & Boys, B. L. (2015). Use of satellite observations for long-term exposure assessment of global concentrations of fine particulate matter. *Environmental Health Perspectives*, *123*(2), 135–143. https://doi.org/10.1289/ehp.1408646

van Geffen, J., Boersma, K. F., Eskes, H., Sneep, M., ter Linden, M., Zara, M., & Veefkind, J. P. (2020). S5P TROPOMI NO_2 slant column retrieval: Method, stability, uncertainties and comparisons with OMI. *Atmospheric Measurement Techniques*, *13*(3), 1315–1335. https://doi.org/10.5194/amt-13-1315-2020

Veefkind, J., Aben, I., McMullan, K., Förster, H., De Vries, J., Otter, G., et al. (2012). TROPOMI on the ESA sentinel-5 precursor: A GMES mission for global observations of the atmospheric composition for climate, air quality and ozone layer applications. *Remote Sensing of Environment*, *120*, 70–83. https://doi.org/10.1016/j.rse.2011.09.027

Vigouroux, C., Langerock, B., Bauer Aquino, C. A., Blumenstock, T., Cheng, Z., De Mazière, M., et al. (2020). TROPOMI-Sentinel-5 Precursor formaldehyde validation using an extensive network of ground-based Fourier-transform infrared stations. *Atmospheric Measurement Techniques*, *13*(7), 3751–3767. https://doi.org/10.5194/amt-13-3751-2020

Wang, S. X., Zhao, B., Cai, S. Y., Klimont, Z., Nielsen, C. P., Morikawa, T., et al. (2014). Emission trends and mitigation options for air pollutants in East Asia. *Atmospheric Chemistry and Physics*, *14*(13), 6571–6603. https://doi.org/10.5194/acp-14-6571-2014

Wei, W., Wang, S., Hao, J., & Cheng, S. (2011). Projection of anthropogenic volatile organic compounds (VOCs) emissions in China for the period 2010–2020. *Atmospheric Environment*, *45*(38), 6863–6871. https://doi.org/10.1016/j.atmosenv.2011.01.013

Wolfe, G. M., Kaiser, J., Hanisco, T. F., Keutsch, F. N., de Gouw, J. A., Gilman, J. B., et al. (2016). Formaldehyde production from isoprene oxidation across NO_x regimes. *Atmospheric Chemistry and Physics*, *16*(4), 2597–2610. https://doi.org/10.5194/acp-16-2597-2016

Xing, C. Z., Liu, C., Hu, Q. H., Fu, Q. Y., Lin, H., Wang, S. T., et al. (2020). Identifying the wintertime sources of volatile organic compounds (VOCs) from MAX-DOAS measured formaldehyde and glyoxal in Chongqing, southwest China. *Science of the Total Environment*, 715. https://doi.org/10.1016/j.scitotenv.2019.136258

Zhang, Z., Wei, M., Pu, D., He, G., Wang, G., & Long, T. (2021). Assessment of annual composite images obtained by Google Earth engine for urban areas mapping using random forest. *Remote Sensing*, *13*(4), 748. https://doi.org/10.3390/rs13040748

Zhao, M., Cheng, W. M., Zhou, C. H., Li, M. C., Wang, N., & Liu, Q. Y. (2017). GDP spatialization and economic differences in South China based on NPP-VIIRS nighttime light imagery. *Remote Sensing*, *9*(7), 673. https://doi.org/10.3390/rs9070673

Zhu, L., González Abad, G., Nowlan, C. R., Chan Miller, C., Chance, K., Apel, E. C., et al. (2020). Validation of satellite formaldehyde (HCHO) retrievals using observations from 12 aircraft campaigns. *Atmospheric Chemistry and Physics*, *20*(20), 12329–12345. https://doi.org/10.5194/acp-20-12329-2020

Zhu, L., Jacob, D. J., Keutsch, F. N., Mickley, L. J., Scheffe, R., Strum, M., et al. (2017). Formaldehyde (HCHO) as a hazardous air pollutant: Mapping surface air concentrations from satellite and inferring cancer risks in the United States. *Environmental Science & Technology*, *51*(10), 5650–5657. https://doi.org/10.1021/acs.est.7b01356

19448007, 2022, 18, Downloaded from https://agupubs.onlinelibrary.wiley.com/doi/10.1029/2022GL099470 by South University Of Science, Wiley Online Library on [11/10/2022]. See the Terms and Conditions (https://onlinelibrary.wiley.com/terms-and-conditions) on Wiley Online Library for rules of use; OA articles are governed by the applicable Creative Commons License

Zhu, L., Jacob, D. J., Mickley, L. J., Marais, E. A., Cohan, D. S., Yoshida, Y., et al. (2014). Anthropogenic emissions of highly reactive volatile organic compounds in eastern Texas inferred from oversampling of satellite (OMI) measurements of HCHO columns. *Environmental Research Letters*, *9*(11), 114004. https://doi.org/10.1088/1748-9326/9/11/114004

Zhu, L., Mickley, L. J., Jacob, D. J., Marais, E. A., Sheng, J., Hu, L., et al. (2017). Long-term (2005–2014) trends in formaldehyde (HCHO) columns across North America as seen by the OMI satellite instrument: Evidence of changing emissions of volatile organic compounds. *Geophysical Research Letters*, *44*(13), 7079–7086. https://doi.org/10.1002/2017GL073859

References From the Supporting Information

Giglio, L., Randerson, J. T., & van der Werf, G. R. (2013). Analysis of daily, monthly, and annual burned area using the fourth-generation global fire emissions database (GFED4). *Journal of Geophysical Research: Biogeosciences*, *118*(1), 317–328. https://doi.org/10.1002/jgrg.20042

Guenther, A. B., Jiang, X., Heald, C. L., Sakulyanontvittaya, T., Duhl, T., Emmons, L. K., & Wang, X. (2012). The model of emissions of gases and aerosols from nature version 2.1 (MEGAN2.1): An extended and updated framework for modeling biogenic emissions. *Geoscientific Model Development*, *5*(6), 1471–1492. https://doi.org/10.5194/gmd-5-1471-2012

19448007, 2022, 18, Downloaded from https://agupubs.onlinelibrary.wiley.com/doi/10.1029/2022GL099470 by South University Of Science, Wiley Online Library on [11/10/2022]. See the Terms and Conditions (https://onlinelibrary.wiley.com/terms-and-conditions) on Wiley Online Library for rules of use; OA articles are governed by the applicable Creative Commons License